Plasmon polaritons in photonic superlattices containing a left-handed material

2009 EPL 88 24002

(http://iopscience.iop.org/0295-5075/88/2/24002)

A Letters Journal Exploring the Frontiers of Physics

October 2009

EPL, **88** (2009) 24002
doi: 10.1209/0295-5075/88/24002

www.epljournal.org

Plasmon polaritons in photonic superlattices containing a left-handed material

E. Reyes-Gómez[1], D. Mogilevtsev[2,3], S. B. Cavalcanti[4(a)], C. A. A. de Carvalho[5,6] and L. E. Oliveira[2,6]

[1] *Instituto de Física, Universidad de Antioquia - AA 1226, Medellín, Colombia*
[2] *Instituto de Física, UNICAMP - CP 6165, Campinas-SP, 13083-970, Brazil*
[3] *Institute of Physics, NASB - F. Skarina Ave. 68, Minsk, 220072, Belarus*
[4] *Instituto de Física, UFAL, Cidade Universitária - 57072-970, Maceió-AL, Brazil*
[5] *Instituto de Física, UFRJ, Rio de Janeiro-RJ - 21945-972, Brazil*
[6] *Inmetro, Campus de Xerém, Duque de Caxias-RJ - 25250-020, Brazil*

received 20 July 2009; accepted in final form 7 October 2009
published online 9 November 2009

PACS 41.20.Jb – Electromagnetic wave propagation; radiowave propagation
PACS 42.70.Gi – Light-sensitive materials
PACS 42.70.Qs – Photonic bandgap materials

Abstract – We analyze one-dimensional photonic superlattices which alternate layers of air and a left-handed material. We assume Drude-type dispersive responses for the dielectric permittivity and magnetic permeability of the left-handed material. Maxwell's equations and the transfer-matrix technique are used to derive the dispersion relation and transmission spectra for the propagation of obliquely incident optical fields. The photonic dispersion indicates that the growth direction component of the electric (or magnetic) field leads to the propagation of electric (or magnetic) plasmon polaritons, for either TE or TM configurations. Furthermore, we show that if the plasma frequency is chosen within the photonic $\langle n(\omega)\rangle = 0$ zeroth-order bandgap, the coupling of light with plasmons weakens considerably. As light propagation is forbidden in that particular frequency region, the plasmon-polariton mode reduces to a pure plasmon mode.

Over the years, artificial complex materials have been increasingly used to shape and manipulate light [1–5]. The micro-structuring of high quality optical materials yields remarkable flexibility in the fabrication of nano-structures, and allows for the tailoring of electromagnetic dispersions and mode structures to suit almost any need. Metamaterials [6–13], also known as left-handed materials (LHMs), are a remarkable example of such nanostructuring. Light propagation through metamaterials is characterized by a phase velocity opposite to the Poyinting vector, which corresponds to negative dispersive electric and magnetic responses.

The advent of metamaterials has opened a new era for optical devices, and has also given considerable thrust to the recent area of plasmonics, the study of plasmon polaritons. In metal-dielectric interfaces, for example, surface-plasmon polaritons are coupled modes that result from resonant interactions between electromagnetic waves and mobile electrons at the surface of a metal or semiconductor. Such resonant surface-plasmon polaritons may have much shorter wavelengths than that of the radiation, which enables them to propagate along nanoscale systems [1–4], opening up a wide range of possibilities for the construction of new optical devices. It is well known, for example, that one of the most important features of surface-plasmon polaritons is to confine light to very small dimensions, yielding the merging of photonics and electronics at the nanoscale. Furthermore, considering the dispersive character of the LHMs, together with the enhanced optical magnetism exhibited by them, one might conjecture the existence of remarkable new phenomena such as the excitation of plasmon polaritons of a magnetic nature, that is, magnetic density waves resulting from resonant interactions between the optical field and the current densities within the metamaterial. Ultimately, those developments could lead to increases in the resolution of microscopes, in the efficiency of LEDs, and in the sensitivity of chemical and biological devices [5–8].

One-dimensional (1D) superlattices which alternate layers of positive and negative materials have already

(a) E-mail: sbessa@gmail.com

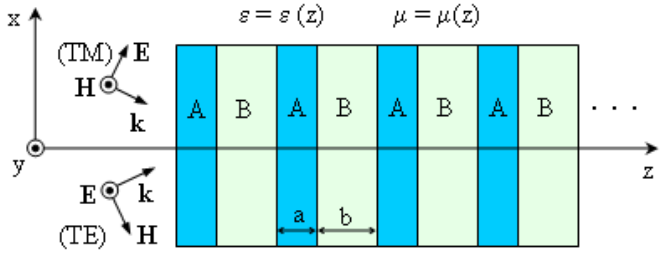

Fig. 1: (Color online) Pictorial view of the 1D multilayer photonic superlattice with layers A and B in periodic arrangement, and the electric and magnetic fields for the TE-like and TM-like electromagnetic waves schematically shown. Note that, for normal incidence, the two polarizations are equivalent.

exhibited many interesting properties [14–23] that are absent in superlattices composed solely of positive materials. In particular, the existence of a non-Bragg photonic bandgap, also known as a zeroth-order gap, has been suggested [12], detected [13,14], and characterized [15,16]. In order to investigate the possibility of excitation of electric/magnetic plasmon polaritons, in the present work we study the oblique incidence of light on a model 1D superlattice composed of layers A of air, and layers B of a doubly negative material. Layers A (width a) and B (width b) are distributed periodically so that $d = a + b$ is the period of the superlattice nanostructure (cf. fig. 1).

In the B layers, the electric and magnetic responses are dispersive and may assume negative values. If one neglects losses, they may be described by [9–13]

$$\epsilon_B(\omega) = \epsilon_0 - \frac{\omega_e^2}{\omega^2}; \qquad \mu_B(\omega) = \mu_0 - \frac{\omega_m^2}{\omega^2}\,, \tag{1}$$

where $\epsilon_B(\omega)$ and $\mu_B(\omega)$ are the dielectric permittivity and magnetic permeability in slab B, respectively, one may choose [10,11] $\epsilon_0 = 1.21$ and $\mu_0 = 1.0$, and the electric/magnetic plasmon modes are at $\nu = \nu_e = \frac{\omega_e}{2\pi\sqrt{\epsilon_0}}$ and $\nu = \nu_m = \frac{\omega_m}{2\pi\sqrt{\mu_0}}$, which correspond to the solutions of $\epsilon_B(\omega) = 0$ and $\mu_B(\omega) = 0$, respectively.

We note that dispersions such as those in (1) hold in periodically LC loaded transmission lines [10]. These negative-index systems were shown to exhibit good microwave properties, with low loss and broad bandwidth [11].

We shall be interested in studying the properties of both the transverse-electric (TE: electric field parallel to the interface plane, see fig. 1) and transverse-magnetic (TM: magnetic field parallel to the interface) polarizations of a monochromatic electromagnetic field of frequency ω propagating through a 1D periodic system.

In the case of a TE field, one may choose

$$\mathbf{E}(\mathbf{r}, t) = E(z)\exp[i\,(qx - \omega t)]\,\mathbf{e}_y, \tag{2}$$

whereas, in the case of TM polarization, the magnetic field may be considered as

$$\mathbf{H}(\mathbf{r}, t) = H(z)\exp[i\,(qx - \omega t)]\,\mathbf{e}_y, \tag{3}$$

where we have assumed that the superlattice was grown along the z-axis, q is the wave vector component along the x-direction, and $\mathbf{e}_y$ is the Cartesian unitary vector along the y-direction.

Maxwell's equations lead to the following differential equations for the electric and magnetic amplitudes:

$$\frac{\mathrm{d}}{\mathrm{d}z}\left[\frac{1}{\mu(z)}\frac{\mathrm{d}}{\mathrm{d}z}E(z)\right] = -\epsilon(z)\left[\left(\frac{\omega}{c}\right)^2 - \frac{q^2}{n^2(z)}\right]E(z), \tag{4}$$

and

$$\frac{\mathrm{d}}{\mathrm{d}z}\left[\frac{1}{\epsilon(z)}\frac{\mathrm{d}}{\mathrm{d}z}H(z)\right] = -\mu(z)\left[\left(\frac{\omega}{c}\right)^2 - \frac{q^2}{n^2(z)}\right]H(z), \tag{5}$$

where $n(z) = \sqrt{\epsilon(z)}\sqrt{\mu(z)}$ is the z-position–dependent refraction index.

In the sequel, n_A and n_B are the refraction indices, while μ_A and μ_B are the magnetic permeabilities in layers A and B, respectively. Note that, because of (1), the n_B refraction index in layer B is a function of the frequency, and may be a real positive, real negative or a pure imaginary number. Also, note that q, the incident wave vector component along the x-direction, may be obtained as a function of the angle of incidence $\theta \equiv \theta_A$ by $q = \frac{\omega}{c} n_A \sin\theta$.

Equations (4) and (5) may be solved by means of the transfer-matrix technique (see, for example, the work by Cavalcanti *et al.* [16] and references therein). For n_B a real number, and $n_B^2 - n_A^2\sin^2\theta \geqslant 0$, the procedure yields the TE polarization dispersion relation from the solution of the transcendental equation

$$\begin{aligned}\cos(kd) \;=\; & \cos(Q_A a)\cos(Q_B b) \\ & -\frac{1}{2}\left(\frac{F_A}{F_B} + \frac{F_B}{F_A}\right)\sin(Q_A a)\sin(Q_B b).\end{aligned} \tag{6}$$

In the formula, k is the Bloch wave vector along the z-direction which is the axis of the photonic crystal; fields in consecutive unit cells are related by the Bloch condition, *i.e.*, by the phase factor $e^{\,i\,k\,d}$. Q_A and Q_B are defined as

$$Q_A = \frac{\omega}{c} n_A |\cos\theta| = \frac{\omega}{c} n_A |\cos\theta_A|, \tag{7}$$

and

$$Q_B = \frac{\omega}{c}\sqrt{n_B^2 - n_A^2\sin^2\theta} = \frac{\omega}{c}|n_B||\cos\theta_B|, \tag{8}$$

where, $F_A = (Q_A/\mu_A)$, $F_B = (Q_B/\mu_B)$ and, in the last equality, we have made use of Snell's law $n_A\sin\theta = n_B\sin\theta_B$.

For n_B a real number, and $n_B^2 - n_A^2\sin^2\theta < 0$, the procedure yields the TE polarization dispersion relation from the solution of the transcendental equation

$$\begin{aligned}\cos(kd) \;=\; & \cos(Q_A a)\cosh(Q_B b) \\ & -\frac{1}{2}\left(\frac{F_A}{F_B} - \frac{F_B}{F_A}\right)\sin(Q_A a)\sinh(Q_B b).\end{aligned} \tag{9}$$

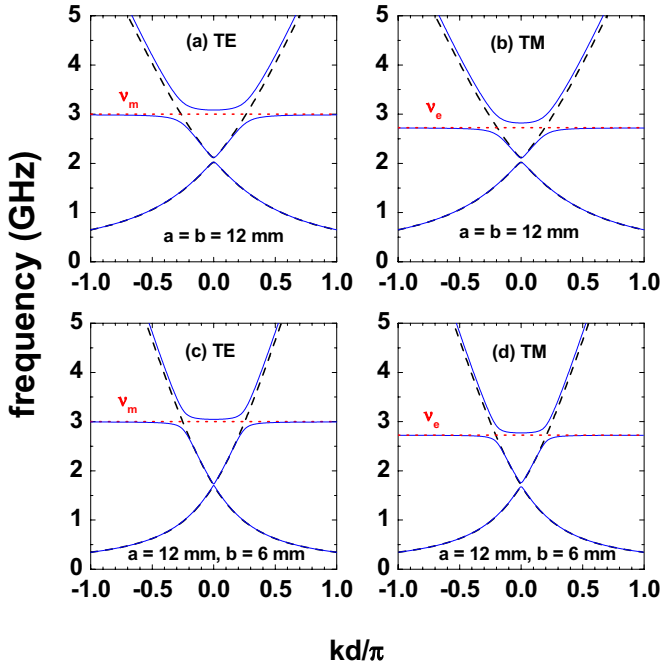

Fig. 2: (Color online) TE and TM dispersion relations $\nu = \nu(k)$ in photonic periodic superlattices ($\nu = \frac{\omega}{2\pi}$). Calculations were performed for air as slab A ($\epsilon_A = 1$, $\mu_A = 1$), $a = b = 12\,\mathrm{mm}$ (also for $a = 12\,\mathrm{mm}$ and $b = 6\,\mathrm{mm}$), and $\omega_e/2\pi = \omega_m/2\pi = 3\,\mathrm{GHz}$ for the Drude model (cf. eq. (1)) in slab B. Dotted lines indicate the pure electric/magnetic plasmon modes at $\nu = \nu_e = \frac{\omega_e}{2\pi\sqrt{\epsilon_0}}$ and $\nu = \nu_m = \frac{\omega_m}{2\pi\sqrt{\mu_0}}$. Solid and dashed lines correspond to $\theta = \pi/12$ and $\theta = 0$ incidence angles, respectively.

where Q_A is still given by (7), but

$$Q_B = \frac{\omega}{c}\sqrt{n_A^2 \sin^2\theta - n_B^2}. \tag{10}$$

Moreover, if $n_B^2 < 0$, (9) is still valid, with Q_A still given by (7), but

$$Q_B = \frac{\omega}{c}\sqrt{n_{BI}^2 - n_A^2 \sin^2\theta}, \tag{11}$$

where n_{BI} is the imaginary part of n_B.

For the TM polarization, the transcendental equations (6) and (9), as well as the definitions of Q_A and Q_B for the different cases are also valid, provided one replaces μ_A by ϵ_A and μ_B by ϵ_B, where ϵ_A and ϵ_B are the dielectric permittivities in layers A and B, respectively.

Figure 2 shows the calculated dispersions ($\nu = \frac{\omega}{2\pi}$) in the cases of TE (figs. 2(a) and (c)) and TM (figs. 2(b) and (d)) polarizations, for different layer widths. Note that ν_e and ν_m fall outside the $\langle n(\omega)\rangle = 0$ zeroth-order bandgap. For $\theta = 0$ (dashed curves), the second shown photonic band, just above the $\langle n(\omega)\rangle = 0$ zeroth-order gap, is a pure photonic mode and, for $\theta = \pi/12$, there is a coupling between the radiation field and a plasmon mode which leads to a pair of plasmon-polariton modes. In other words, while for normal incidence the band just above the zeroth-order gap is a pure photonic mode,

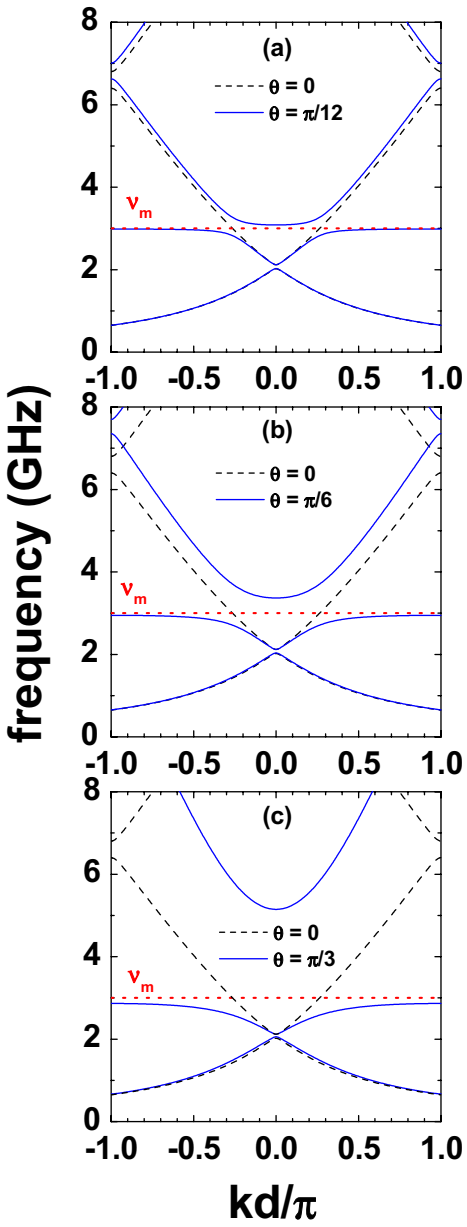

Fig. 3: (Color online) TE dispersion relations $\nu = \nu(k)$ in $a = b = 12\,\mathrm{mm}$ photonic periodic superlattices ($\nu = \frac{\omega}{2\pi}$) as functions of various incidence angles. Here, dotted lines indicate the pure magnetic plasmon modes at $\nu = \nu_m = \frac{\omega_m}{2\pi\sqrt{\mu_0}}$. Dashed lines correspond to $\theta = 0$ and solid lines correspond to (a) $\theta = \pi/12$, (b) $\theta = \pi/6$ and (c) $\theta = \pi/3$ incidence angles, respectively.

for oblique incidence ($\theta \neq 0$) the *electromagnetic field + plasmon* interaction leads to a pair of coupled modes. We emphasize that, for $\theta = 0$, the electric- and magnetic-field components along the z growth direction are null and there is no longitudinal wave propagation. On the other hand, for $\theta \neq 0$, in the case of the TM (TE) configuration, the electric (magnetic) field has a component on the z-direction, which results in the excitation of longitudinal electric (magnetic) waves. For $\theta = \pi/12$, fig. 2 illustrates that the pair of plasmon-polariton bands are asymptotic

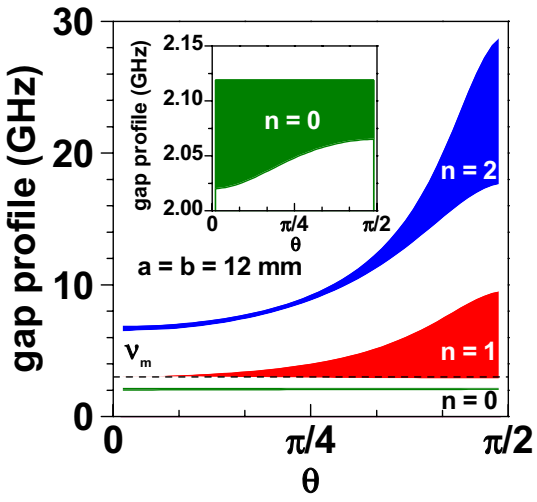

Fig. 4: (Color online) Gap profiles for TE waves as functions of the angle of incidence in a photonic periodic superlattice (with $a = b = 12\,\text{mm}$). The $\langle n \rangle = 0$ zeroth-order gap is labeled as $n = 0$ and is shown in detail in the inset to illustrate its behavior with the θ incidence angle. The plasmon-polariton gap is labeled as $n = 1$ and the Bragg gap at the boundary is denoted as $n = 2$. The dashed line indicates the pure magnetic plasmon mode at $\nu = \nu_m = \frac{\omega_m}{2\pi\sqrt{\mu_0}}$.

to the $\nu = \nu_e$ and $\nu = \nu_m$ pure electric/magnetic plasmon values. It is clear from fig. 2(a), for example, that at small values of k, the lowest $\theta = \pi/12$ plasmon-polariton mode behaves like an electromagnetic photonic wave. As k increases, the dispersion bends over and reaches the limiting value of the pure magnetic plasmon. On the other hand, the second $\theta = \pi/12$ plasmon-polariton branch behaves like a magnetic plasmon wave, at small k, and like an electromagnetic photonic mode as k increases. The same comments are valid for the other panels in fig. 2 (of course, in the cases of figs. 2(b) and (d), the electric plasmon mode is the one involved). By comparing the results for normal and oblique incidence, it is clear that, for $\theta \neq 0$, resonant plasmon-polariton waves are excited by the coupling of the electric (or magnetic) plasmon modes with the incident eletromagnetic field. One may infer that the plasmon-polariton waves are excited by the magnetic field, in the TE case, or driven by the electric field, in the TM case. This is consistent with the fact that those longitudinal waves, in the TE case, are asymptotic to the ν_m pure magnetic plasmon frequency whereas, in the TM case, the plasmon-polariton bands are asymptotic to the ν_e pure electric plasmon mode.

The calculated dispersions, for TE modes, as a function of the incidence angle are displayed in fig. 3. We notice that the essential features persist irrespective of the incidence angle, although both the plasmon-polariton gap and Bragg gap at the boundary widen considerably for higher incidence angles, as expected. Figure 4 depicts the gap profiles for TE waves as functions of the incidence angle for $a = b = 12\,\text{mm}$. One clearly sees that the $\langle n \rangle = 0$ zeroth-order gap (labeled as $n = 0$) is not omnidirectional

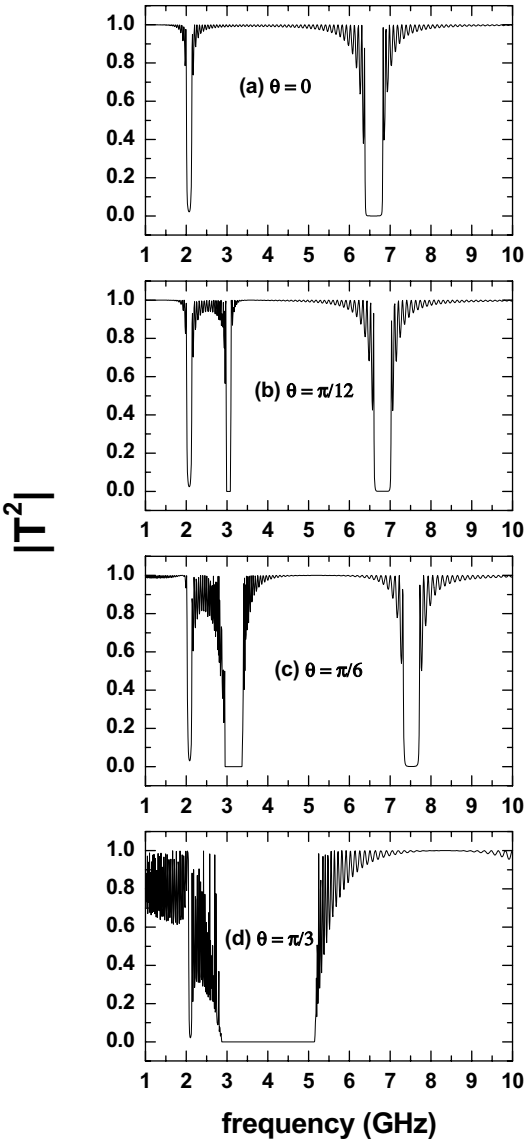

Fig. 5: Transmission plots of TE waves, as functions of the angle of incidence, through a stack of 50 unit cells composed of air as slab A ($\epsilon_A = 1$, $\mu_A = 1$) with length $a = 12\,\text{mm}$, and slab B, with length $b = 12\,\text{mm}$, as a LHM with electric/magnetic responses given by the Drude model (*i.e.*, a stack of 50 unit cells corresponding to the same superlattice as in fig. 3).

and decreases with increasing incidence angle. Also, the plasmon-polariton gap (labeled as $n = 1$) and the Bragg gap at the boundary (denoted as $n = 2$) increase as the angle of incidence increases. Figure 5 illustrates the transmission spectra for a stack composed of fifty unit cells, with $a = b = 12\,\text{mm}$. Null transmission results should be compared with the corresponding gaps in figs. 3 and 4. It is clear, therefore, that calculated transmission spectra corroborate the results obtained for the corresponding infinite photonic periodic superlattice via the dispersion relation (cf. figs. 3 and 4).

Furthermore, fig. 6 clearly indicates that, by choosing the resonant plasmon frequency within the $\langle n(\omega) \rangle = 0$

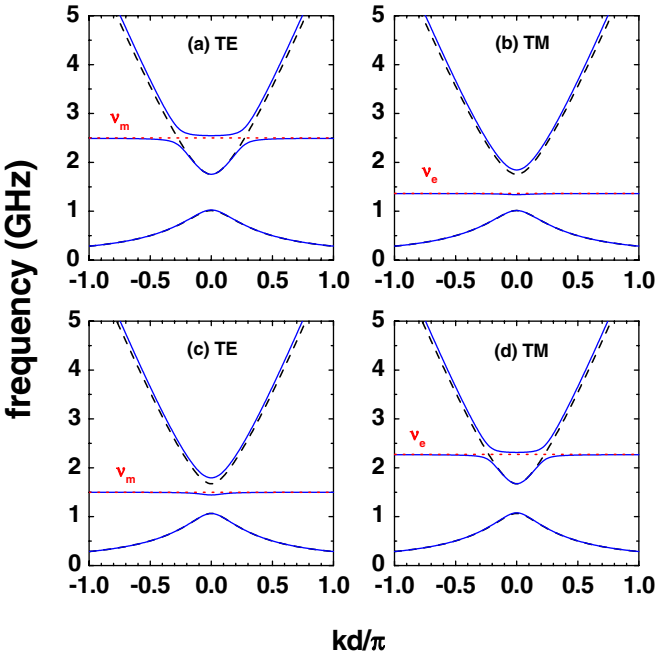

Fig. 6: (Color online) TE and TM dispersions in a photonic periodic superlattice with $a = b = 12\,\text{mm}$. Numerical calculations were carried out for air as slab A ($\epsilon_A = 1$ and $\mu_A = 1$). For slab B, ϵ_B and μ_B were chosen by taking plasma frequencies in the Drude model as $\omega_e/2\pi = 1.5\,\text{GHz}$ and $\omega_m/2\pi = 2.5\,\text{GHz}$, respectively, in (a) and (b), whereas in (c) and (d) we have taken $\omega_e/2\pi = 2.5\,\text{GHz}$ and $\omega_m/2\pi = 1.5\,\text{GHz}$. Note that, in panel (b), the electric plasmon frequency $\nu_e = \frac{\omega_e}{2\pi\sqrt{\epsilon_0}}$ is in the $\langle n(\omega)\rangle = 0$ zeroth-order bandgap region, leading to a basically flat $\theta = \pi/12$ plasmon-polariton band with a frequency essentially equal to ν_e for the TM dispersion. A similar situation is observed for the TE dispersion in (c), as $\nu_m = \frac{\omega_m}{2\pi\sqrt{\mu_0}}$ falls in the zeroth-order gap region. Solid and dashed lines correspond to $\theta = \pi/12$ and $\theta = 0$ incidence angles, respectively.

zeroth-order bandgap, the coupling of light to plasmon modes, for $\theta \neq 0$, essentially disappears leading to a basically pure (electric or magnetic) plasmon mode. This is a consequence of the fact that the energy of the incident electromagnetic wave lies in a forbidden energy gap region and, therefore, the coupling of the incident light with plasmons is expected to be quite weak.

Here we note that the present study has dealt with a 1D superlattice containing an isotropic LHM layer. Nevertheless, it is important to point out that the realization of isotropic LHM systems is still a great experimental challenge, and that available LHM structures are mostly anisotropic [24–27]. Of course, a proper consideration of the effects of an anisotropic electric/magnetic response for the LHM layer would bring additional complexities in the present theoretical approach. We do not expect, however, that the essential physics of the present study —on the plasmon polaritons in photonic superlattice containing left-handed materials with isotropic responses— would change in any substantive way.

In conclusion, we have studied light propagation through a 1D superlattice composed of alternate layers of a positive constant material and a negative dispersive material, and verified the appearance of coupled plasmon-polariton modes of electric and magnetic nature. The photonic dispersion was calculated from Maxwell's equations using the transfer-matrix approach, with the LHM modeled by Drude-like dielectric and magnetic responses. In the case of oblique $\theta \neq 0$ incidence, the photonic dispersion indicates that the magnetic or electric field in the frequency region around the $\langle n(\omega)\rangle = 0$ zeroth-order bandgap leads to coupled magnetic or electric plasmon-polariton modes for the TE and TM configurations, respectively. Moreover, present results show that the coupling of light with plasmons is weakened by choosing the plasma frequency inside the zeroth-order gap. As light propagation is forbidden in that particular gap-frequency region, the coupled plasmon-polariton mode becomes essentially a pure plasmon mode. This feature permits one to select which type of plasmon polariton (*i.e.*, electric or magnetic) one is willing to excite, by choosing the magnetic or electric plasmon frequency within the zeroth-order gap. The possibility of magnetic plasmon-polariton excitations should provide a new look towards the implementation of novel techniques and devices based on the interplay of photonics and magnetism at the nanoscale, similarly to the interplay of photonics and electronics [28,29]. There are still practical challenges to be dealt with in such systems, such as the challenge of reducing loss which is the common problem related to metamaterials. Here, we have studied an ideal system neglecting losses which, one could argue, may taint the coupling in such a way as to hinder plasmon-polariton excitations. However, a study on an anisotropic bilayer composed of well balanced positive and negative materials reveals that, compared to a single isotropic meta layer, the influence of loss on the behavior of the transfer function, for various transverse wave vector k_x, is greatly reduced [24]. On the other hand, considering that classical electrodynamics predicts a substantially lower radiation loss of a magnetic dipole than the radiation loss of an electric dipole of a similar size [30], one might conjecture that the combination of anisotropic stacks with plasmons of a magnetic origin should serve as a quite good model towards practical implementations such as magnetic plasmonic chips for high data rate processing or sensing applications. Future experimental and theoretical studies on layered systems including loss effects and anisotropy are certainly forthcoming.

* * *

We thank A. Bruno-Alfonso for stimulating discussions, and are grateful to the Brazilian Agencies CNPq, FAPESP, FAPERJ, and FUJB, the Colombian Agency COLCIENCIAS, and CODI - University of Antioquia for partial financial support.

REFERENCES

[1] Shelby R. A., Smith D. R. and Schultz S., *Science*, **292** (2001) 77.
[2] Barnes W. L., Dereux A. and Ebbesen T. W., *Nature*, **424** (2003) 824.
[3] Maier S. A. and Atwater H. A., *J. Appl. Phys.*, **98** (2005) 011101.
[4] Ramakrishna A., *Rep. Prog. Phys.*, **68** (2005) 449.
[5] Ozbay E., *Science*, **311** (2006) 189.
[6] Dolling G., Enkrich C., Wegener M., Soukoulis C. M. and Linden S., *Opt. Lett.*, **31** (2006) 1800.
[7] Li T., Li J.-Q., Wang F.-M., Wang Q.-J., Liu H., Zhuy S.-N. and Zhu Y.-Y., *Appl. Phys. Lett.*, **90** (2007) 251112.
[8] Dragoman M. and Dragoman D., *Prog. Quantum Electron.*, **32** (2008) 1.
[9] Pacheco J. jr., Grzegorczyk T. M., Wu B.-I., Zhang Y. and Kong J. A., *Phys. Rev. Lett.*, **89** (2002) 257402.
[10] Eleftheriades G. V., Iyer A. K. and Kremer P. C., *IEEE Trans. Microwave Theory Tech.*, **50** (2002) 2702.
[11] Grbic A. and Eleftheriades G. V., *J. Appl. Phys.*, **92** (2002) 5930; Liu L., Caloz C., Chang C. C. and Itoh T., *J. Appl. Phys.*, **92** (2002) 5560.
[12] Li J., Zhou L., Chan C. T. and Sheng P., *Phys. Rev. Lett.*, **90** (2003) 083901.
[13] Jiang H., Chen H., Li H., Zhang Y. and Zhu S., *Appl. Phys. Lett.*, **83** (2003) 5386.
[14] Smith D. R., Padilla W. J., Vier D. C., Nemat-Nasser S. C. and Schultz S., *Phys. Rev. Lett.*, **84** (2000) 4184.
[15] Liscidini M. and Andreani L. C., *Phys. Rev. E*, **73** (2006) 016613.
[16] Cavalcanti S. B., Dios-Leyva M., Reyes-Gómez E. and Oliveira L. E., *Phys. Rev. B*, **74** (2006) 153102; *Phys. Rev. E*, **75** (2007) 026607; Bruno-Alfonso A., Reyes-Gómez E., Cavalcanti S. B. and Oliveira L. E., *Phys. Rev. A*, **78** (2008) 035801.
[17] Shadrivov I. V., Sukhorukov A. A. and Kivshar Y. S., *Appl. Phys. Lett.*, **82** (2003) 3820.
[18] Ziolkowski R. W., *Phys. Rev. E*, **70** (2004) 046608.
[19] Daninthe H., Foteinopoulou S. and Soukoulis C. M., *Photonics Nanostruct. Fundam. Appl.*, **4** (2006) 123.
[20] Yuan Y., Ran L., Huangfu J., Chen H., Shen L. and Kong J. A., *Opt. Express*, **14** (2006) 2220.
[21] Vasconcelos M. S., Mauris P. W., de Medeiros F. F. and Albuquerque E. L., *Phys. Rev. B*, **76** (2007) 165117.
[22] Weng Y., Wang Z.-G. and Chen H., *Phys. Rev. E*, **75** (2007) 046601.
[23] Zhang L., Zhang Y., He L., Wang Z., Li H. and Chen H., *J. Phys. D: Appl. Phys.*, **40** (2007) 2579.
[24] Smith R. and Schurig D., *Phys. Rev. Lett.*, **90** (2003) 077405.
[25] Wang S. and Gao L., *Eur. Phys. J. B*, **48** (2005) 29.
[26] Sun S., Huang X. and Zhou L., *Phys. Rev. E*, **75** (2007) 066602.
[27] Han P., Chan C. T. and Zhang Z. Q., *Phys. Rev. B*, **77** (2008) 115332.
[28] Liu H., Li T., Wang Q. J., Zhu Z. H., Wang S. M., Li J. Q., Zhu S. N., Zhu Y. Y. and Zhang X., *Phys. Rev. B*, **79** (2009) 024304.
[29] Liu H., Liu Y. M., Li T., Wang S. M., Zhu S. N. and Zhang X., *Phys. Status Solidi B*, **246** (2009) 1397.
[30] Jackson J. D., *Classical Electrodynamics* (Wiley, New York) 1999.